Supporting Information

Yu et al. 10.1073/pnas.1119577109

SI Materials and Methods

PCR, Quantitative PCR, and RT-PCR. Mitochondrial and nuclear fractions isolated from cells or ocular tissues were pooled. DNA was extracted from each fraction with the DNeasy blood and tissue kit (Qiagen). Delivery of human ND4 was analyzed by PCR assay with primer hND4F1, 5′-ATGCTAAAACTAATCGTCC-3′; hND4R1403, 5′-CTCTTGTCATCGTCGTCC-3′. Quantitative PCR assay with oligonucleotides F1, 5′-TTCCTATTCTACACCCTACTCATTACTATTCTGCCTA-3′, and R1, 5′-TAGTCATATTAAGTTATTGGCGTAGAGTTTGAAGTCCTT-3′, for human ND4; oligonucleotides F2, 5′-TTCATCCTTCTCTCCCTA-3′, and R2, 5′-ATTATTAGTATTGTTGCTCCTAT-3′, for mouse ND4; oligonucleotides F3, 5′-CATTGTTGGTCCATACGG-3′, and R3, 5′-TGCTAGTGTGAGTGATAGG-3′, for mouse ND1; and oligonucleotides F4, 5′-AGAACACCTCTGATTACTCCT-3′, and R4, 5′-TTCGGTTGGTCTCTGCTA-3′, for human ND1. DNA integration was detected with the first round of the PCR assay with forward primer human ND4F629, 5′-CGGACTCCACTTATGACTCC-3′, plus the following three reverse primers: P1 (mouse mtDNA R 11626), 5′-ATGGAAGCATGAATTAGC-3′; P2 (mouse mtDNA R 11687), 5′-GGTTCCTAAGACCAATGG-3′; and P3 (mouse mtDNA R 11593), 5′-TCTTGGTGAATAAGGAGG-3′. DNA integration was detected with the second round of the PCR assay with primer human ND4F, 5′-CGAACGCACTCACAGTCACATCATAATCCTCTCTC-3′, and P3, 5′-TCTTGGTGAATAAGGAGG-3′. Total RNA was isolated from transfected or infected cells or from mouse optic nerves and retinas (n = 10) (RNeasy Protect Mini Kit; Qiagen). RT-PCR was performed with an RT-PCR system (Access; Promega): human ND4-primer, 5′-ATTCTCATCCAAACCCCCTGAAGCTT-3′, and antisense primer, 5′-TTGTCATCGTCGTCCTTGTAGTCAG-3′,with an expected PCR product size of 500 bp; and human ATP8 primer F, 5′-CCATACTCCTTACACTATTCC-3′, and R, 5′-GCAATGAATGAAGCGAAC-33′, with an expected PCR product size of 150 bp. Resultant PCR products were electrophoresed on a 1% agarose gel and stained with ethidium bromide.

We used sense primer 5′-ATGCTAAAACTAATCGTCCCAACAATTAT-3′ and antisense primer 5′-TGTCGGGGTTGAGGGATAGG-3′ for amplification of full-length human *ND4*. For amplification of the HSP or FLAG region unique to our construct, we combined the respective *ND4* primers with 5′-TAACCCCATACCCCGAACCAACCAAACCCCAAAGACAC-3′ (HSP) primer or 5′-TTGTCATCGTCGTCCTTGTAGTCAG-3′ primer (FLAG) to give a ∼1.4-kb product. For RT-PCR, we used the FLAG antisense primer with ND4 5′-GCCCTCGTAGTAACAGCCATTCT-3′ to give a 500-bp product.

For Southern blotting, the extracted mtDNA was digested with NdeI, electrophoresed on a 0.7% agarose gel, and then transferred to the blotting membrane with the Trans-Blot SD System according to the manufacturer's instructions (Bio-Rad). The human ND4FLAG fragment from 921 to 1,405 bp was prepared from sc-HSP-*ND4FLAG*, digested by BamHI and HindIII, and used as a probe. The probe labeling and hybridization were done with the digitonin high prime DNA labeling and detection starter kit II according to the manufacturer's instructions (Roche).

ATP Assay. The rate of ATP synthesis was measured by chemiluminescence with a modified luciferin-luciferase assay in digitonin-permeabilized cells with the complex I substrates malate and pyruvate in real time with an Optocom I luminometer (MGM Instruments) and expressed per milligram of protein. For the ATP-based cell viability assay, the infected cells were selected in galactose media for 5 d and then grown in standard glucose media to the desired confluence. Cells were then seeded in 96-well plates at 5,000 cells per well and cultured in galactose or glucose media for 5 d. On each day, the number of viable cells was tested based on quantitation of ATP present using the CellTiter-Glo luminescent cell viability assay according to the manufacturer's instructions (Promega). The ATP luminescence in restrictive galactose media was assessed as a percentage of that of the corresponding culture grown in standard glucose media.

Animals. All animal procedures were performed in accordance with the National Institutes of Health Guide for Care and Use of Laboratory Animals and the Association for Research in Vision and Ophthalmology (ARVO) statement for the use of Animals in Ophthalmic and Vision Research. For the intraocular injection of recombinant AAV, DBA/1J mice were sedated by inhalation with 1.5–2% isoflurane. A local anesthetic (proparacaine HCl) was applied topically to the cornea, and a 32-gauge needle attached to a Hamilton syringe was then inserted through the pars plana. One microliter of scAAV2/COX8VP2*ND4FLAG* (1.01×10^{11} VG/mL), scAAV2/VP2*ND4FLAG*, allotopic mutant ND4 ssAAV2/R340H-*ND4* (1.08×10^{11} VG/mL), or scAAV-*GFP* (1.03×10^{12} VG/mL) was injected into the vitreous body.

For detection of WT ND4 import, transcription, and translation, mice were injected with AAV2/VP2COX8GFP/sc-HSP-*ND4FLAG*, AAV2 VP2/sc-*HSP-ND4*, or scAAV2-*GFP* in both eyes. Animals were killed at certain time points after injection. DNA and RNA were extracted from the retina or optic nerve.

For the 1-mo rescue experiments, 10 mice were injected intravitreally with AAV2/VP2COX8GFP/sc-HSP-*ND4FLAG* into the right eyes and scAAV2-*GFP* into the left eyes. Another 10 mice were injected with AAV2/VP2/sc-HSP-*ND4FLAG* into the right eyes and scAAV2-*GFP* into the left eyes. To induce optic neuropathy, both eyes were injected vitreally 2 d later with ssAAV2/R340H-*ND4FLAG*.

For the 3- to 12-mo rescue experiments, we had a total of 30 mice and both eyes were injected vitreally with 1 μL of AAV2/VP2COX8GFP/sc-HSP-*ND4FLAG* (n = 10), AAV2/VP2/sc-HSP-*ND4FLAG* (n = 10), or scAAV2-*GFP* (n = 10). Both eyes in each of these 30 mice were then injected vitreally 2 d later with ssAAV2/R340H-*ND4* to induce optic neuropathy. As an additional control, we injected the left eyes of 10 mice with only scAAV-*GFP*.

PERG. In brief, mice were weighed and anesthetized with i.p. injections of a mixture of ketamine (80 mg/kg of body weight) and xylazine (10 mg/kg of body weight), and were restrained by using a bite bar and a nose holder that allowed unobstructed vision. The animals were kept at a constant body temperature of 37.6 °C with a feedback-controlled heating pad. In these conditions, the eyes of mice were wide open and in a stable position with undilated pupils pointing laterally and upward. The electroretinogram electrode had a diameter of 0.25 mm and was made of silver wire configured to a semicircular loop with a 2-mm radius; it was placed on the corneal surface by means of a micromanipulator and positioned in such a way as to encircle the pupil without limiting the field of view. Reference and ground electrodes were stainless-steel needles inserted under the skin of the scalp and tail, respectively. After setting the mice on the stage and before recording, a small drop of balanced saline was topically applied on the cornea to prevent drying. A visual stimulus of contrast-reversing bars (50° × 58° field

area, mean luminance of 50 cd/m^2, spatial frequency of 0.05 cycles per degree, contrast of 100%, and temporal frequency of 1 Hz) was aligned with the projection of the pupil at a distance of 20 cm. Eyes were not refracted for the viewing distance because the mouse eye has a large depth of focus as a result of the pinhole pupil. Retinal signals were amplified (10,000-fold) and band pass-filtered (1–30 Hz). Three consecutive responses to 600 contrast reversals each were recorded. The responses were superimposed to check for consistency and then averaged. The PERG is a light-adapted response. To have a corresponding index of outer retinal function, a light-adapted flash electroretinogram (FERG) was also recorded with undilated pupils in response to strobe flashes of 20 cd·m^2·s superimposed on a steady background light of 12 cd/m^2 and presented within a Ganzfeld bowl. Under these conditions, rod activity is largely suppressed, whereas cone activity is minimally suppressed. Averaged PERGs and FERGs were automatically analyzed to evaluate the major positive and negative waves by Sigma Plot (Systat Software, Inc.).

Histology and Ultrastructure. At the appropriate time points, rodents inoculated with the AAV vectors were overdosed with sodium pentobarbital. They were perfused by cardiac puncture with PBS and then with fixative consisting of 4% paraformaldehyde in 0.1 M PBS buffer (pH 7.4) or, for detection of in vivo H_2O_2, with a mixture consisting of 2 mM cerium chloride, 10 mM 3-amino-1,2,4-triazole, 0.8 mM NADH, 0.1 M PBS buffer (pH 7.5), and 7% sucrose, followed by perfusion with the fixative. The eyes with attached optic nerves were dissected out and further processed by immersion fixation in 2.5% glutaraldehyde; postfixed in 1% osmium tetroxide, 0.1 M sodium cacodylate-HCl buffer (pH 7.4), and 7% sucrose in the cold; and then dehydrated through an ethanol series to propylene oxide, infiltrated, and embedded in epoxy resin that was polymerized at 60 °C overnight. For immunocytochemistry, tissue specimens were postfixed in 5.0% acrolein, 0.1 M sodium cacodylate-HCl buffer (pH 7.4), and 7% sucrose, and then dehydrated through an ethanol series and embedded in LR White (Ted Pella, Inc.) that was polymerized at 50 °C overnight. Semithin longitudinal sections (0.5 μm) of the optic nerve head and retrobulbar nerve were stained with toluidine blue for light microscopic examination. Ultrathin sections (90 nm) were placed on nickel grids for immunocytochemistry with anti-FLAG antibodies, MnSOD antibodies, or A20 antibodies counterstained by secondary antibodies conjugated to 5 nm of immunogold; the gold particles were then amplified with a silver enhancement kit (Ted Pella, Inc.). Examinations were made with an H-7600 transmission electron microscope (Hitachi) with a tilting stage for 3D rendering of collected images or an H-7650 transmission electron microscope (Hitachi), operating at 120 or 80 kV, respectively.

Optic Nerve Diameters and Axon Counts. One year after viral gene injections, optic nerves were dissected from ~1 mm behind the globe to the optic chiasm. The diameter of each optic nerve was an average of 10 measurements covering the entire orbital and intracranial optic nerve. Images were captured with a video camera mounted on a dissection microscope at a magnification of 10×. After specimen preparation, toluidine blue-stained images were collected using an Olympus IX50 microscope, equipped with an Olympus DP7e CCD camera (Olympus America). For axon counts, five transmission electron micrographs were photographed at low magnification (2,500×) for each optic nerve specimen. The number of axons was then manually counted by an observer masked to the treatment agent. Axons were identified by the internalized neurotubules and axolemma surrounded by an electron-dense myelin sheath. Axons counts were expressed per square millimeter and then multiplied by the total area for each optic nerve.

Statistical Analysis. Values were expressed as the mean ± SD. Data were analyzed via the Student t test for paired data. $P < 0.05$ was considered as significant, and $P < 0.01$ was considered as highly significant.

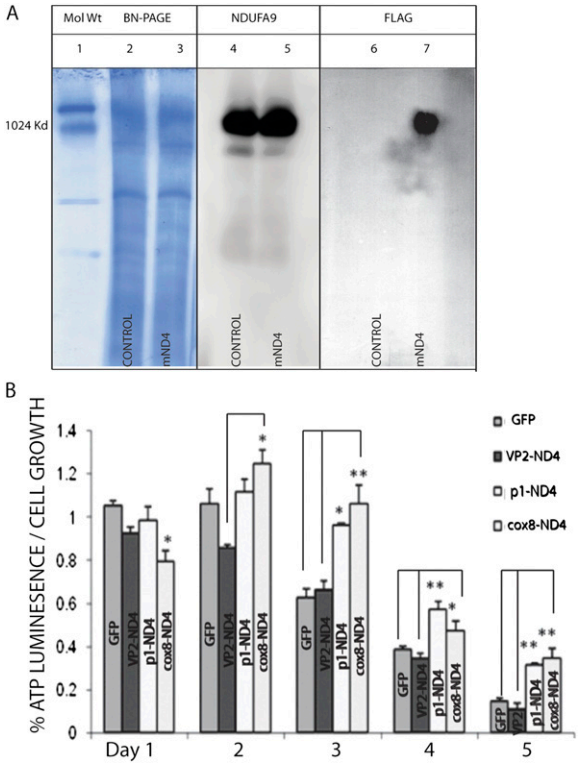

Fig. S1. (*A*) 1D BN/PAGE gel shows that the large ~1,000-kDa complex I band is evident in the blue native gel for control (lane 2) and MTS AAV ND4FLAG-infected cells (lane 3). Immunoblotting of the transferred proteins stained for the nuclear-encoded NDUFA9 subunit of complex I shows NDUFA9 signal in both uninfected (lane, 4) and infected (lane 5) mitochondrial pellets. Although a FLAG signal is not visualized in mitochondrial pellets of uninfected cells (lane 6), a FLAG signal is seen in MTS AAV-infected mitochondria (lane 7). Lane 1 is the molecular weight standards. (*B*) Bar plot of ATP luminescence shown as a percentage of cell survival in restrictive media to cell growth in normal glucose media revealed no differences 1 d after infection with AAV-GFP (GFP) lacking ND4FLAG, VP2 AAV lacking the MTS but carrying the ND4FLAG, the allotopic nuclear-encoded ND4FLAG, or the MTS AAV containing the mitochondrial ND4FLAG cDNA gene. On day 2, differences in ATP levels between cybrids rescued with COX8GFP VP2-delivered ND4 (cox8-ND4) started to show significance relative to untargeted VP2-ND4 (brackets) (**P* = 0.05). On day 3, ATP levels were highest with MTS AAV ND4FLAG infection and significantly greater than infection with AAV-GFP or with VP2 ND4 lacking the MTS (brackets) (***P* = 0.001). On day 4, ATP levels with COX8-ND4 rescue were greater than those infected with AAV-GFP or VP2-ND4, being highly significant (brackets) (***P* = 0.001). On day 5, ATP levels were highest with COX8-ND4 treatment, with differences between this construct and those infected with AAV-GFP or VP2-ND4 being highly significant (brackets) (***P* = 0.001). Comparison with rescue with the allotopic nuclear-encoded version of *ND4* (p1-ND4) is also shown but not bracketed. Although differences between ATP levels of p1-ND4–infected cells were significantly greater than those infected with AAV-GFP or VP2-ND4 (***P* = 0.001) at days 4–5, differences between p1-ND4 and cox8-ND4 were not significant.

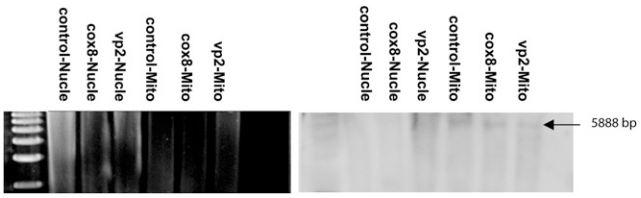

Fig. S2. Southern blot with the human ND4 fragment from 921–1,405 bp used as the probe shows an ~6-kb band in Nde1-digested mtDNA isolated from mouse retinas injected with COX8 VP2 AAV (COX8-Mito), VP2 without the MTS (VP2-Mito) AAV, or AAV-GFP (control) as well as in the nuclear fragment isolated from retinas injected with VP2 without the MTS AAV (VP2-Nucle). No bands are seen in the nuclear fraction isolated from COX8 VP2 (COX 8-Nucle) AAV-injected retinas or in the AAV-GFP–injected controls (control-Nucle).